UNVEILING THE IMPACT OF AIR CHANGE RATES ON PARTICLE DISPERSION IN PATIENT WARDS

Sien Jie Wong[a,b], Huiyi Tan[c], Hong Yee Kek[a], Mohd Hafiz Dzarfan Othman[d], Poj Tangamchit[e], Maria Anityasari[f], Norfazira Abdullah[a], Muhammad Faiz Hilmi Rani[a], Keng Yinn Wong[a,b]*

[a]Faculty of Mechanical Engineering, Universiti Teknologi Malaysia, 81310 UTM Johor Bahru, Johor, Malaysia.
[b]Process System Engineering Centre (PROSPECT), Universiti Teknologi Malaysia, 81310 UTM Johor Bahru, Johor, Malaysia.
[c]Faculty of Chemical and Energy Engineering, Universiti Teknologi Malaysia, 81310 UTM Johor Bahru, Johor, Malaysia.
[d]Advanced Membrane Technology Research Centre (AMTEC), Universiti Teknologi Malaysia, 81310 UTM Johor Bahru, Johor, Malaysia.
[e]Department of Control Systems and Instrumentation Engineering, King Mongkut's University of Technology Thonburi, 10140 Bangkok, Thailand.
[f]International Office Institut Teknologi Sepuluh Nopember, Institut Teknologi Sepuluh Nopember, 60111 Jawa Timur, Indonesia.

*Corresponding email: kengyinnwong@utm.my

Article history
Received
4th April 2025
Revised
12th May 2025
Accepted
13th May 2025
Published
1st December 2025

ABSTRACT

The purpose of this study is to examine the effect of air change rate (ACH) on reducing particle concentration in a patient ward using numerical simulation. A patient ward is a large room or space in a medical facility where individuals with similar health conditions or treatments are grouped. It is equipped with modern beds, medical care systems, lighting, and ventilation systems to maintain a high level of hygiene. Airborne transmission in patient wards can easily spread to other individuals. Therefore, the ACH in the patient ward needs to be increased. Three ACH cases were investigated along with a baseline case using a simplified CFD model. The patient ward model was constructed and validated based on past literature. The Renormalization Group (RNG) k-epsilon turbulence model was selected to simulate airflow velocity in the patient ward. The movement of airborne particles was simulated using the Discrete Phase Model (DPM). An effective ACH was determined from the three cases. Based on the results, the most effective ACH in reducing particle dispersion in the patient ward was identified. The findings indicate that in Case 3, where ACH = 25h^{-1} and the ventilation opening size was 1 m × 1 m, the high airflow velocity in the patient ward completely reduced airborne particle concentration (100%) above patient 1 and 100% around other patients and medical staff. By reducing particle concentration, the number of particles that could infect other patients was also significantly reduced.

Keywords: *Air Change Rates, Particle Dispersion, Patient Wards*

©2025 Penerbit UTM Press. All rights reserved

1.0 INTRODUCTION

A healthcare facility provides medical, preventive, or rehabilitative care to individuals with illness. In some cases, the patients need to stay in patient wards for medical supervision

and treatment. The patients in the wards have weakened immune systems, making them more vulnerable to infections caused by airborne bacteria, viruses, and mold spores, as well as direct contact with healthcare workers and contaminated surgical or medical equipment [1]. The risk of infection in patient wards remains significant due to the presence of asymptomatic infections and the incubation period of various pathogens [2]. Among all the pathogens, *Clostridioides difficile* (*C. difficile*), *Staphylococcus aureus* (*S. aureus*), and *Klebsiella* are the most common causes of hospital-acquired infections (HAIs), also known as nosocomial infections, accounting for 12.1%, 10.7%, and 9.9% of cases, respectively [3]. The situation worsens when inpatient care facilities, such as general medical and surgical hospitals, are used simultaneously by patients, medical staff, and visitors, making them highly susceptible to HAIs [4].

Research conducted in Nebraska, USA, found that 63 % of air samples collected from inpatient wards and hallway air tested positive [5]. In this context, medical staff are also highly vulnerable to viral infections and other emerging diseases due to their close contact with infected patients and exposure to contaminated materials [6]. The exposure risk of medical staff varies across different hospital departments, with high-risk departments showing a 55% positive rate, respiratory departments reporting a 38% positive rate, and specialist medicine departments having a 8.6% positive rate [7]. The higher positive rates in high-risk and respiratory departments indicate increased exposure to airborne pathogens due to frequent interactions with infected patients and procedures that generate aerosols. In contrast, the lower positive rate in specialist medicine suggests a comparatively lower risk of transmission in those areas.

Another threat comes from airborne transmissible infections. When an infected person coughs, sneezes, talks, or breathes, they release respiratory droplets and aerosols into the air. These particles can remain suspended for extended periods and travel long distances before being inhaled by others, potentially causing infection. Occupants may also contribute to the spread of airborne pathogens by transporting them through their clothes or resuspending particulate matter (PM) and microbial materials from the floor [8]. Respiratory infections can spread through droplets of different sizes. Three main transmission routes, namely droplet, fomite and aerosol are accountable for the transmission incidents in an enclosed environment [9]. Studies have shown that PM2.5 is closely associated with various pathogenic bacteria [10] whereas 94% of PM10 composition is dominated by bacteria [11]. The airflow pattern was thought to play a vital role in several epidemics of airborne infectious diseases in hospital wards [12]. Poorly ventilated areas allow infectious particles to accumulate, increasing transmission risk. The spread of the SARS coronavirus (SARS-CoV) during Hong Kong's largest nosocomial SARS outbreak, along with the recent outbreak of Middle East Respiratory Syndrome (MERS) in South Korean hospitals, demonstrated that airborne disease transmission due to inefficient hospital ward ventilation systems can lead to serious health risks [12, 13]. Poor ventilation significantly increases the risk of virus transmission in inpatient wards, primarily through contact and airborne pathways.

To reduce airborne transmission caused by poor ventilation, ensuring an adequate air supply and efficient exhaust systems is essential, as proper airflow plays a crucial role in controlling particle dispersion. Optimizing ventilation within patient wards is therefore vital in minimizing the spread of airborne viruses. Hospital heating, ventilation, and air conditioning (HVAC) systems are specifically designed to create a safe and comfortable indoor environment while effectively controlling the spread of infectious particles. Among the various IAQ parameters, air exchange rate or air change per hour (ACH) plays a pivotal role in determining how effectively airborne particles are diluted, dispersed, and removed within enclosed spaces, such as patient wards. A low ACH means that the volume of fresh air introduced into the space per hour is limited, resulting in a lower dilution effect and increased microbial count [14, 15]. When the air exchange rate is insufficient, pollutants, including airborne pathogens and particulate matter, remain suspended in the indoor

environment for longer periods, increasing the risk of infection and exposure. Removing recirculated air and increasing ACH are effective measures for reducing long-range indirect inhalation exposure [7]. A minimum of 5 ACH is recommended to reduce the risk of exposure to airborne pollutants and surgical site infections [16]. Previous studies suggest that increasing ACH from 2 to 8 reduces the risk of particle inhalation by nearly 70 % [17]. By minimizing recirculated air, the concentration of airborne contaminants is reduced, preventing the accumulation and redistribution of infectious particles within the indoor environment. This process decreases the residence time of infectious aerosols, thereby lowering the risk of long-range airborne transmission and improving overall indoor air quality.

Although it is often considered that raising the ACH reduces infection risks, it has been demonstrated that more excellent ventilation rates can increase the risk of pathogen exposure in some circumstances [18]. Ventilation systems drive air from the patient areas to the circulation areas of patient ward. As a result, airborne diseases can move from a ward compartment to the entire ward, potentially leading to nosocomial outbreaks. The design of a ventilation system is a determinant influencing pollutant flow pathways [19]. Hospitals equipped with sophisticated mechanical ventilation systems, featuring higher ACH, good directional airflow, and effective filtration systems, can maintain lower indoor bioaerosol concentrations compared to hospitals relying on natural ventilation systems [20]. These advanced mechanical systems ensure better control over air circulation, pollutant removal, and the prevention of airborne contamination, significantly reducing the risk of infection transmission within hospital environments. The operation and maintenance of ventilation systems are also crucial for maintaining IAQ in hospitals [8]. Poorly maintained and inefficient ventilation systems, with contaminated ductwork and air supply, have been shown to facilitate the transmission of airborne infectious pathogens within hospital indoor environments [21].

Previous studies have established a direct link between ventilation rates and the dispersion of airborne particles [7, 14, 15]. Despite extensive research on HVAC systems and IAQ control, the specific impact of varying ACH on particle behavior in real-world patient wards remains insufficiently explored. With the emergence of novel airborne pathogens and the ongoing challenges of managing respiratory disease outbreaks, a deeper understanding of ACH and its influence on particle dynamics is crucial. While many studies focus on generalized ventilation strategies or idealized environments, they often overlook the complexity of patient wards, which involve unique layouts, varying occupancy levels, and diverse airflow patterns. This gap in knowledge creates uncertainty in optimizing ventilation strategies for effective infection control, highlighting the need for further investigation. Addressing this knowledge gap is paramount to enhancing patient safety and minimizing HAIs. The objective of this research is to examine the effect of ACH on reducing the particle dispersion distance in the patient ward by using numerical simulation. Computational Fluid Dynamics (CFD) simulation will be utilized to study the airflow distribution and particle dispersion in the patient ward based on its high precision and reliability to simulate complex airflow pattern [22]. The outcome of research aims to provide actionable insights for healthcare facility designers and policymakers. The findings could contribute to the development of evidence-based ventilation guidelines tailored to diverse clinical scenarios

2.0 METHODOLOGY

2.1 Constructing and Discretizing CFD Model of the Patient Ward.

In the present study, the patient ward with dimensions 7.5 m × 6.0 m × 2.7 m (length × width × height), accommodates six patients, one medical staff member, and six beds with

dimensions 2.1 m x 0.95 m x 0.5 m (length × width × height) was studied. The ward model was adapted from Satheesan, Mui [23], while the manikin dimensions were based on the work of Kamar, Wong [24]. The spacing between beds is 1.16 m. The ward operates entirely on mechanical ventilation, featuring four ceiling-mounted air supply diffusers, each measuring 0.6 m × 0.6 m, with a total area of 0.36 m² per diffuser. Contaminated air is expelled through eight near-floor-level exhaust outlets, each with dimensions of 0.45 m × 0.25 m (length × height). Figure 1 shows the baseline CFD model of patient ward illustrating the layout of beds and patient positions with the description of manikin dimension.

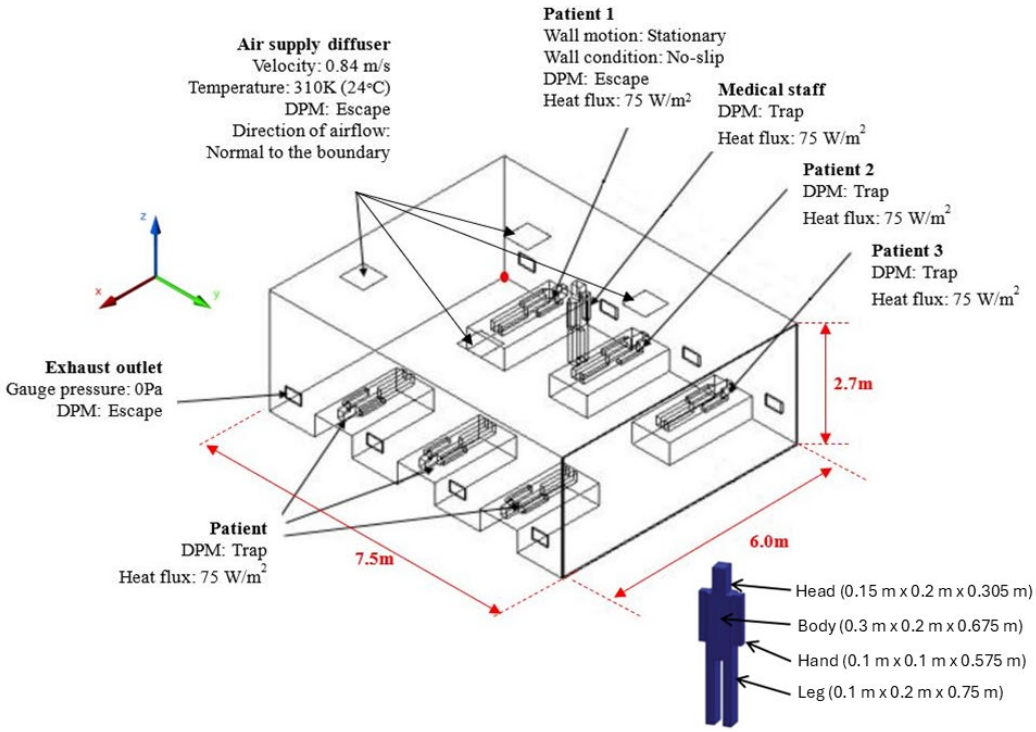

Figure 1: Baseline CFD model of the patient ward showing the arrangement of patients and bed positions.

ANSYS Fluent was used to perform CFD simulations in this study. Various element types are available for discretising the 3D model of computational domain, including tetrahedral, polyhedral, and hexahedral meshes. Each has distinct advantages depending on the geometry, accuracy requirements, and computational efficiency. Tetrahedral elements are widely used for their adaptability in meshing complex and irregular geometries, though they may require more elements for accuracy [25]. Polyhedral elements offer improved numerical stability and faster convergence by providing more neighbouring faces per element [26]. Hexahedral elements, on the other hand, deliver superior accuracy in structured domains and are ideal for boundary-layer modelling [27]. In the present study, an unstructured tetrahedral mesh was utilized to discretize the patient ward in the CFD model, as this type of element is well-suited for capturing complex geometries and ensuring reliable results [28-30]. In the near-wall region, five additional layers were applied using a growth rate of 1.2 to gradually increase the cell size away from the wall. This controlled layering helps to capture near-wall flow behaviour and ensures a smooth transition to the core mesh.

To conduct a grid independence test (GIT) and determine the grid convergence index (GCI), five different mesh densities were tested, ranging from 0.5 million to 8 million

elements. The GIT was performed by doubling the mesh size for each successive set. To monitor GIT fluctuations, a Z-Z line was selected, connecting the coordinates (3.35, 2.50, 1.00) and (3.35, 2.50, 5.00). This line was chosen because it passes through a critical region near the air supply diffuser, which exhibits a high airflow velocity gradient. Figure 2 shows the GIT results, based on 100 evenly distributed sampling points along the Z-Z line.

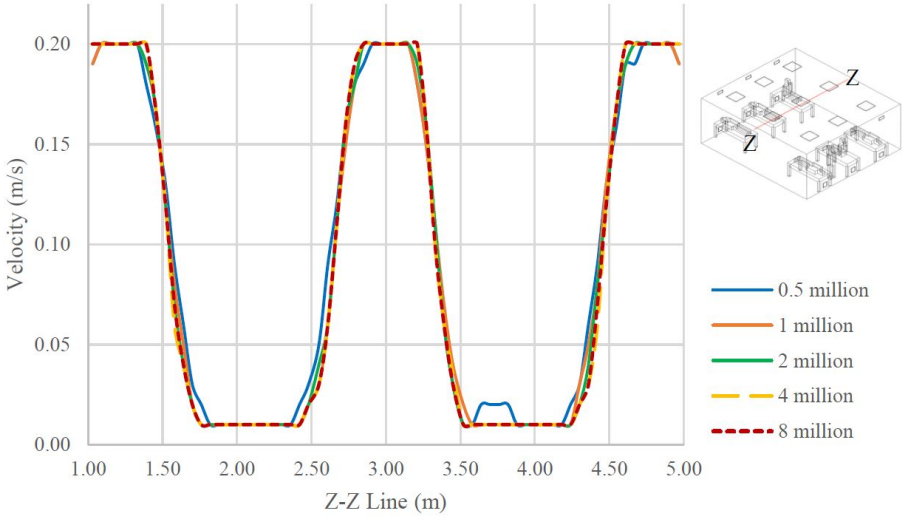

Figure 2: The airflow velocity distribution along Z-Z line in 6-bed patient ward.

Referring to Figure 2, airflow velocity fluctuations become negligible for mesh densities of 1 million elements or more. To ensure the mesh density is sufficiently refined, the GCI should be less than 5% [31]. In this study, the calculated GCI values for mesh sizes of 0.5 million, 1 million, 2 million, and 4 million elements are 29.45%, 12.73%, 6.34%, and 2.62%, respectively. Thus, a 4-million-element mesh is selected for subsequent simulations, as it meets the recommended discretization error threshold of less than 5%. The GCI is computed via Equation (1):

$$\mathrm{GCI(u)} = \frac{F_S \varepsilon_{rms}}{r^p - 1} \tag{1}$$

where F_s is the safety factor, ε is the relative difference between succeeding solutions, p is the order of convergence, and r is the refinement factor between the fine and coarse grid. The ε_{rms} can be defined as in Equation (2) [32]:

$$\varepsilon_{rms} = \sqrt{\frac{\sum_{i=1}^{n} \left(\frac{u_{i,coarse} - u_{i,fine}}{u_{i,fine}}\right)^2}{n}} \tag{2}$$

where u_i is the airflow velocity and n is the number of points measured. The Semi-Implicit Method for Pressure-Linked Equations (SIMPLE) algorithm was chosen to solve the pressure-velocity coupling in the simulation. Its effectiveness in accurately computing the fundamental governing equations has been well-documented in past study [33]. The second-order upwind discretization scheme was selected to minimize numerical diffusion in the solution, in order to enhance the accuracy of the simulated results. The residual error for all conservation equations was set to 1×10^{-6}, while for the energy equation, it was set to 1×10^{-9}. These thresholds help minimize numerical errors and enhance solution accuracy. To accurately capture particle locations, particle trajectories were tracked at every fluid flow iteration instead of the default setting of every 20 iterations. The convergence of the

Discrete Phase Model (DPM) was assessed by monitoring particle deposition on the patient surface under steady-state conditions. Specifically, the mass-weighted average of deposited particles on the patient surface was tracked across iterations. Convergence was achieved once the deposited particle mass stabilized, with no significant fluctuations observed over successive iterations. This approach ensures that particle trajectories and deposition outcomes remain consistent and are not influenced by ongoing changes in the flow field. DPM convergence was reached prior to the continuous phase equations meeting their residual targets, indicating that particle behaviour had already stabilized within the flow field. The analysis also incorporated the spherical drag law within the DPM, which applies the same drag force as a spherical particle while improving the accuracy of drag force predictions in indoor airflow simulations.

2.2 Obtaining Boundary Conditions using Onsite Measurement and Validating Airflow Velocity.

Validation on airflow was being performed in a confined controlled space. The room temperature was maintained at 24°C by operating the air conditioning system for two hours before the onsite measurements. Airflow velocity from each supply diffuser was measured five times to determine the average velocity. The process of onsite measurement samplings was shown in Figure 3(a). An anemometer was positioned at ten locations with a height of 0.9 m, with three recordings taken at each location to calculate the average airflow velocity. Turbulence models were validated by computing the relative error between the experimental and simulated airflow velocity. To be comparable to the actual condition, the percentage of relative error should be less than 10% [28]. The percentage of relative errors was computed using Equation (3):

$$\text{Relative error (\%)} = \frac{|V_{simulated} - V_{experimental}|}{V_{experimental}} \, x \, 100\% \qquad (3)$$

Variation of airflow velocities recorded and simulated using four different turbulence models (standard k-epsilon, RNG k-epsilon, Realizable k-epsilon and Standard k-omega) is shown in Figure 3(b).

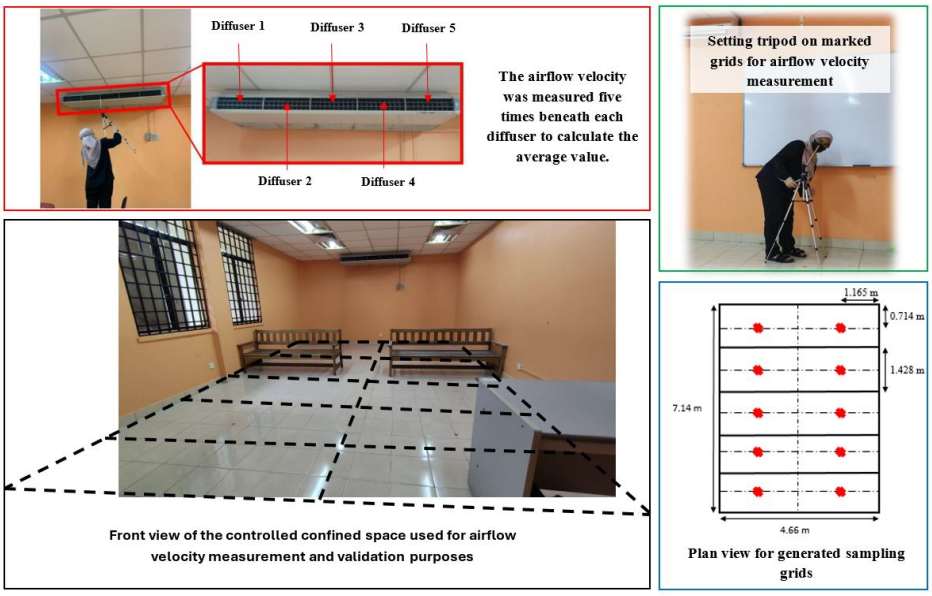

(a)

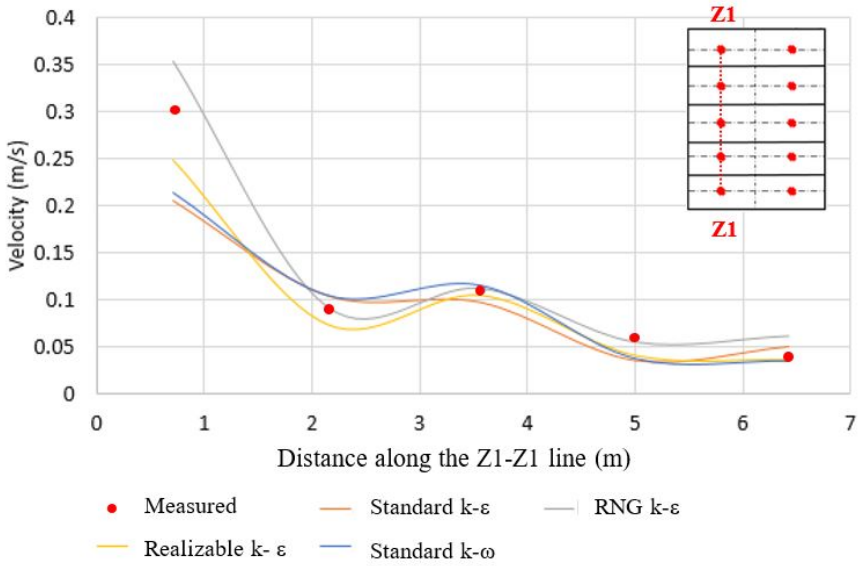

(b)

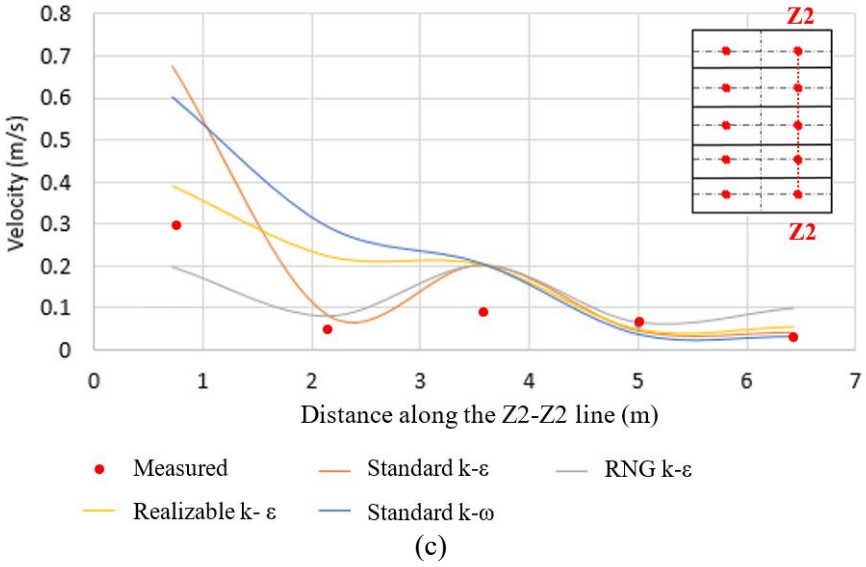

(c)

Figure 3: (a) Onsite measurement samplings in controlled confined space; Variation of airflow velocities along (b) Z1-Z1 line, and (c) Z2-Z2 line.

RNG k-epsilon recorded the lowest percentage relative error (19.3%) along line Z1-Z1 and line Z2-Z2, followed by Standard k-omega (21.4%), Realizable k-epsilon (23.3%) and Standard k-epsilon (26.0%). To select the appropriate turbulence model, the relative error should be less than 10% hence it can be rated as a validated turbulence model with good accuracy [28]. The inaccurate relative error was caused by experimental inconsistencies, including improper placement of the prop, which obstructed airflow and prevented accurate velocity measurements. Additionally, errors in reading and interpreting the results contributed to the overall inaccuracy.

For the particle model's boundary condition, the velocity inlet and pressure outlet were set as escape conditions, consistent with the setup for Patient 1, 2, and 3. The trap condition was applied to the patient, medical staff, and the walls. The flow rate of particles emitted by Patient 1, 2, and 3 was 6.62×10^{-13} kg/s. Neither the patient nor the medical staff engaged

in any intensive activities within the ward. Airborne particles may settle on their clothing and subsequently re-enter the environment. Additionally, clothing fibres are released into the indoor air, as they are considered a source of particulate emissions from the human body. A particle emission rate of 0.5 micrometres was selected based on [34]. The detailed boundary conditions were presented in Table 1. Figure 4 illustrates the mesh configuration of the CFD model.

Table 1: Detailed boundary conditions prescribed on the patient's ward.

Object	Type	Setup
Supply diffuser	Inlet velocity	Velocity magnitude: 0.84 m/s Temperature: 310K (24 °C) DPM: Escape Direction of airflow: Normal to the boundary Turbulent intensity: 5%
	Outlet Pressure	Gauge pressure: 0% DPM: Escape Turbulent intensity: 5%
Medical staff	Wall	Wall motion: Stationary wall Wall condition: No slip DPM: Trap Heat flux: 75 W/m3
Patient 1-3	Wall	Wall motion: Stationary wall Wall condition: No slip DPM: Escape Heat flux: 75 Mass flow rate: 6.62×10^{-13} kg/s
Other patients	Wall	Wall motion: Stationary wall Wall condition: No slip DPM: Trap Heat flux: 75

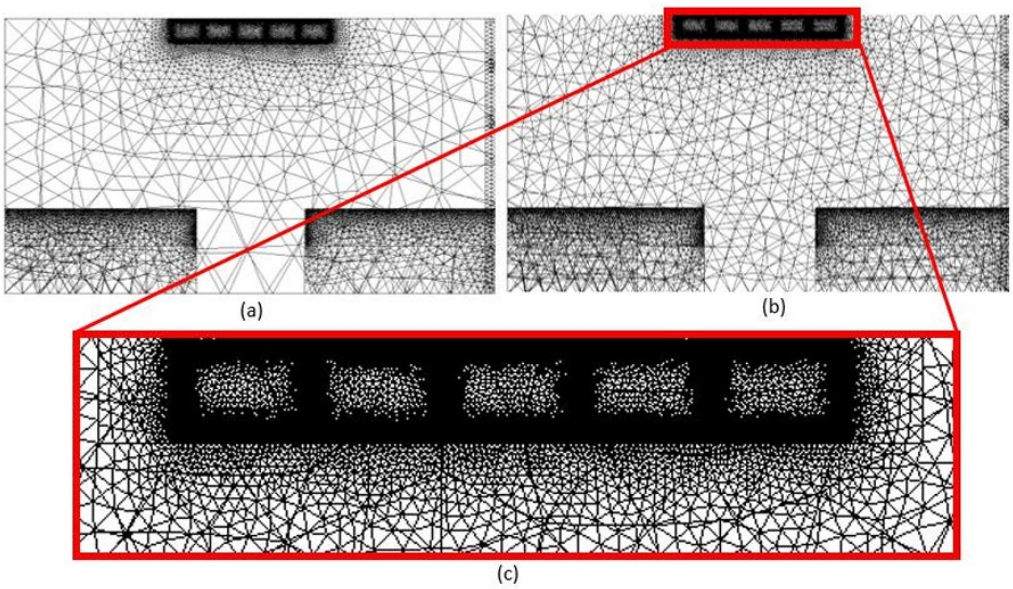

Figure 4: Mesh configurations: (a) Coarse mesh with approximately 0.5 million elements, (b) Fine mesh with approximately 8 million elements, and (c) zoomed-in view highlighting the use of unstructured tetrahedral elements around critical regions of the model.

2.3 Proposing the Effective ACH in Reducing the Particle Dispersion in Patient Ward.

The baseline model includes four air diffusers and eight exhaust grills, strategically positioned near the patient's head with dimensions of 0.45 m × 0.25 m. In the cases studied, the number of supply diffusers increases from four to six with constant inlet airflow velocity of 0.84 m/s, while the exhaust grills remain constant. Case 1 features an ACH of $9h^{-1}$ with diffusers measuring 0.6 m × 0.6 m. In Case 2, the ACH increases to $16h^{-1}$, accompanied by larger diffusers of 0.8 m × 0.8 m. Case 3 further elevates the ACH to $25h^{-1}$, utilizing the largest diffusers at 1 m × 1 m. The key variations across the cases lie in the ACH levels and manipulated diffuser sizes, while the exhaust configuration remains unchanged.

3.0 RESULTS AND DISCUSSION

3.1 Airflow Distribution under Baseline Case.

The baseline model was designed with an inlet air velocity of 0.84 m/s, directed perpendicularly from the supply diffuser. Each case examined the dispersion of airborne particles released from three different patients, Patient 1, Patient 2, and Patient 3. In a 6-bed patient ward with a symmetrical layout, the study focuses only on patients 1-3 on one side because the design and environmental conditions are assumed to be identical on both sides of the room. Since the layout is symmetric, the factors affecting patient conditions such as airflow, ventilation, and air distribution are expected to behave similarly for patients 1-3 on one side as for patients 4-6 on the other side. This approach simplifies the study while still allowing for generalizations based on the symmetry of the ward's design.

Figure 5 presents the airflow velocity vector plot at the XY plane. The color gradient from blue to yellow indicates varying airflow velocities, with blue representing lower velocities and yellow-green indicating higher velocities. Airflow is not uniformly distributed across the ward, suggesting variations in ventilation effectiveness for different patient locations. Certain regions appear to have low airflow velocity (darker blue areas), which could indicate zones where airborne particles may linger longer, increasing the risk of pathogen accumulation. The overall air flow pattern suggests recirculation zones, where air may not be effectively replaced, particularly near beds and corners. Figure 5(a) illustrates the airflow behavior when particles were released from Patient 1. Upon contact, the airflow split into two distinct streams: one directed towards the wall and the other moving downward toward the floor and the medical staff's legs, both with a velocity of 0.21 m/s. The presence of medical staff creates noticeable disturbances in the airflow, potentially affecting how airborne contaminants spread. Figure 5(b) illustrates the airflow pattern when particles were released from Patient 2. Similar to the first case, the airflow divided into two directions: one stream traveled toward the medical staff, while the other moved toward Patient 3 before eventually flowing into the corridor, maintaining a velocity of 0.21 m/s. Figure 5(c) demonstrates the airflow distribution when particles were released from Patient 3. In this case, the velocity vector was noticeably lower than in the previous scenarios, indicating weaker airflow movement.

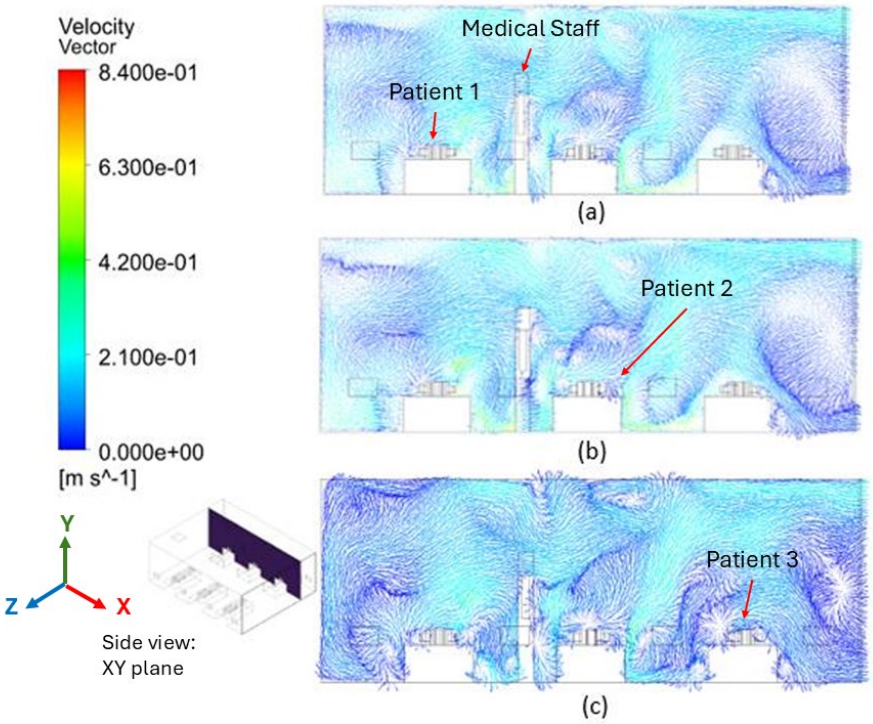

Figure 5: Airflow velocity vector plot when particles are released from (a) Patient 1, (b) Patient 2 and (c) Patient 3.

3.2 Particle Dispersion under Baseline Case.

Particle dispersion involving particle release settings from Patient 1 to Patient 3 was studied accordingly. Figure 6(a) indicated that some airborne particles reached Patient 1's left hand and the nearby medical staff, with concentrations ranging from 11 to 16 particles/m³. The highest particle concentration was observed on the body surface, reaching approximately 53 particles/m³. The side view shows particles staying near the patient level, suggesting limited vertical movement. Some dispersion occurs towards the lower part of the room, indicating settling or movement due to airflow patterns. Figure 6(b) illustrates the dispersion of airborne particles from Patient 2. Similar to Patient 1, high particle concentrations are localized near the patient and medical staff. Some airborne particles appear to spread horizontally, meaning airflow may carry contaminants toward adjacent beds. The particles primarily traveled toward Patient 3 due to the presence of an outlet positioned to the left of Patient 3. Particle concentrations near Patient 2's leg ranged between 32 and 53 particles/m³, while concentrations of 5 to 11 particles/m³ reached Patient 3. Lower particle concentrations trapped around Patient 3 indicate a lower cross infection risk compared to particle release settings from Patient 1. The side view shows slightly higher vertical dispersion compared to Patient 1, possibly due to stronger air currents. Figure 6(c) depicted the particle concentration around Patient 3. Particle dispersion is relatively less intense compared to (a) and (b). A more even distribution of lower concentration particles is seen, suggesting dilution due to air mixing. The side view indicates some particles being carried upwards, possibly due to the ventilation system influence. Approximately 53 particles/m³ accumulated near the body, with 21 to 37 particles/m³ dispersing into the corridor. Notably, Patient 3's airborne particles did not contribute to cross-infection, as the airflow carried them directly toward the corridor.

Observations across these figures suggested that airborne particles originating from Patient 1 posed the highest risk, as they were responsible for the highest concentration

spread contaminating both other patients and medical staff. Medical staff working in areas with high particle accumulation (near Patients 1 and 2) may have increased exposure risk.

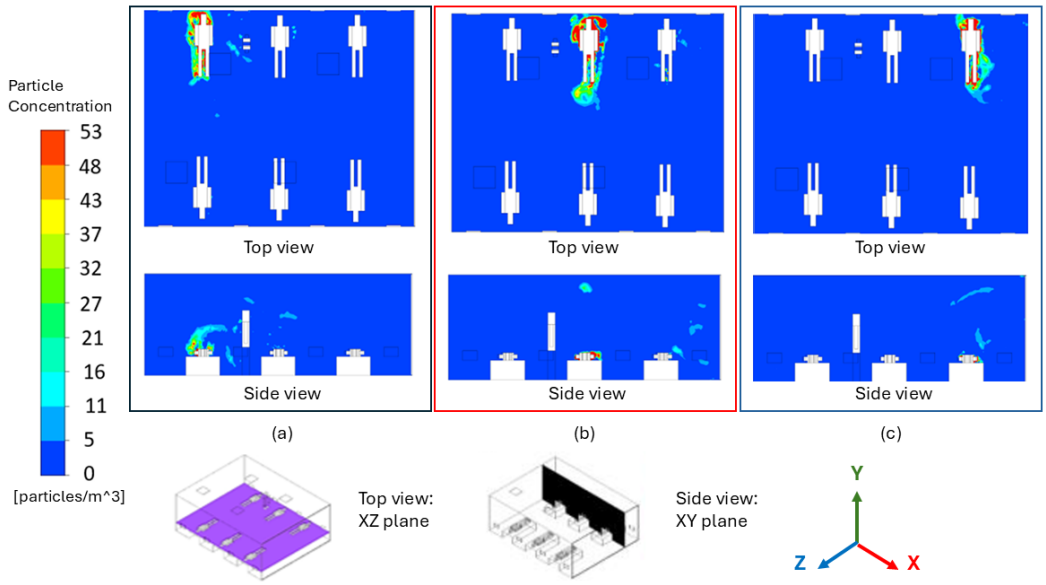

Figure 6: Particle distribution plot when particles are released from (a) Patient 1, (b) Patient 2 and (c) Patient 3.

3.3 Case Study: Impact of ACH on Airflow Distribution and Particle Dispersion

The XY plane was selected to analyse the distribution of airflow velocity, providing a cross-sectional view of the airflow dynamics. This plane intersects both the patient and medical staff at x = 0.9 m, allowing for a detailed examination of airflow behaviour within the ward. Figure 7 illustrates the velocity vector distribution under different inlet supply diffuser configurations, highlighting variations in airflow behavior.

Case 1 recorded the weakest airflow distribution, with limited penetration of airflow into the ward. Air velocity is low near patient areas, meaning poor ventilation efficiency and potential accumulation of contaminants. High stagnation zones, increasing the risk of airborne pathogen retention. The simulated airflow velocity upon impact with patients was 0.63 m/s, while the velocity near the bed and floor measured 0.42 m/s. Case 2 shows a stronger and more evenly distributed airflow compared to Case 1 which leads to better air mixing, reducing stagnant zones and enhancing dilution effects. The airflow striking the patients increased to 0.84 m/s, while the velocity near the floor and medical staff reduced to 0.63 m/s. Case 3 demonstrated the highest air velocity with well-distributed airflow throughout the ward. Strong downward airflow penetration ensures rapid removal of airborne contaminants, minimizing pathogen accumulation. The incoming air at 0.84 m/s split into two directions upon reaching the floor and wall, each with a velocity of approximately 0.63 m/s. The increased supply diffuser size contributed to higher airflow velocities in all cases compared to the baseline scenario, where the airflow velocity was only 0.21 m/s. Among the cases analyzed, Case 3 exhibited the most significant airflow impact, creating a wider and more evenly distributed air movement across the patient ward. In contrast, Cases 1 and 2 showed similar airflow patterns but with progressively lower velocity magnitudes and a more confined airflow distribution. These findings suggest that higher ACH can improve airflow coverage, enhance airborne particle removal, and ultimately contribute to better ventilation efficiency within the patient ward.

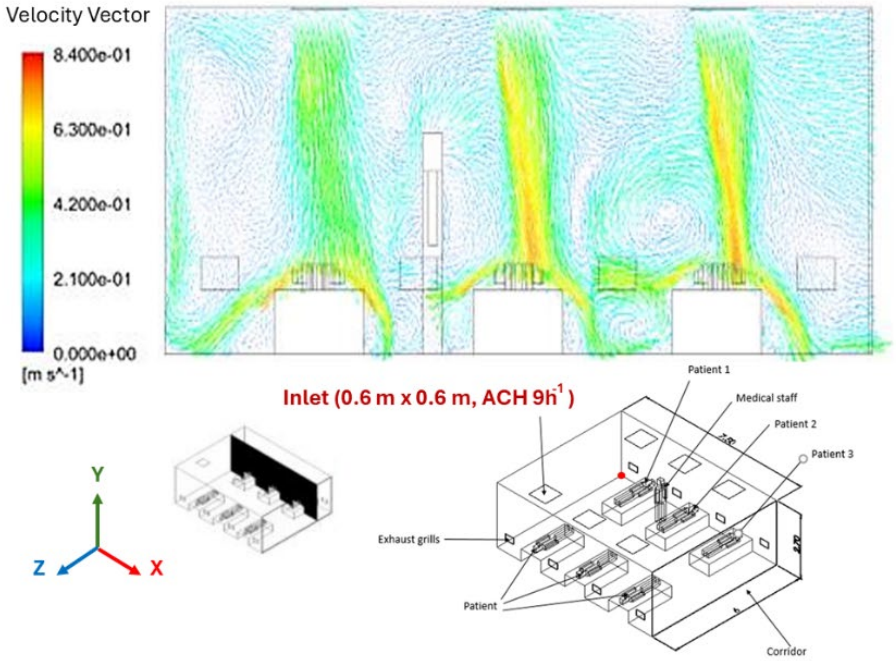
Velocity Vector
8.400e-01
6.300e-01
4.200e-01
2.100e-01
0.000e+00
[m s^-1]
Inlet (0.6 m x 0.6 m, ACH 9h-1)
Y
Z
X
Patient 1
Medical staff
Patient 2
Patient 3
Exhaust grills
Patient
Corridor

(a)

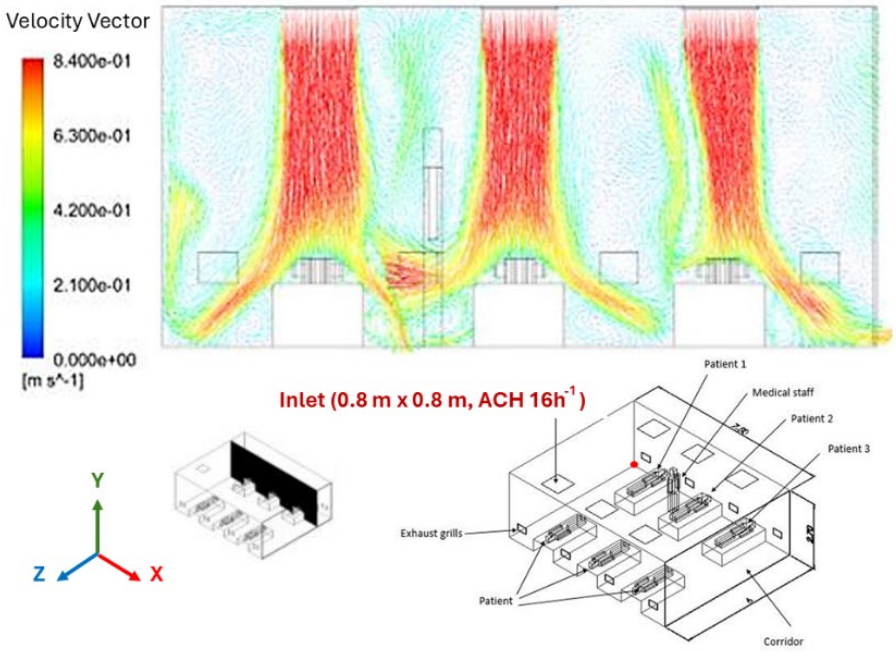
Velocity Vector
8.400e-01
6.300e-01
4.200e-01
2.100e-01
0.000e+00
[m s^-1]
Inlet (0.8 m x 0.8 m, ACH 16h-1)
Y
Z
X
Patient 1
Medical staff
Patient 2
Patient 3
Exhaust grills
Patient
Corridor

(b)

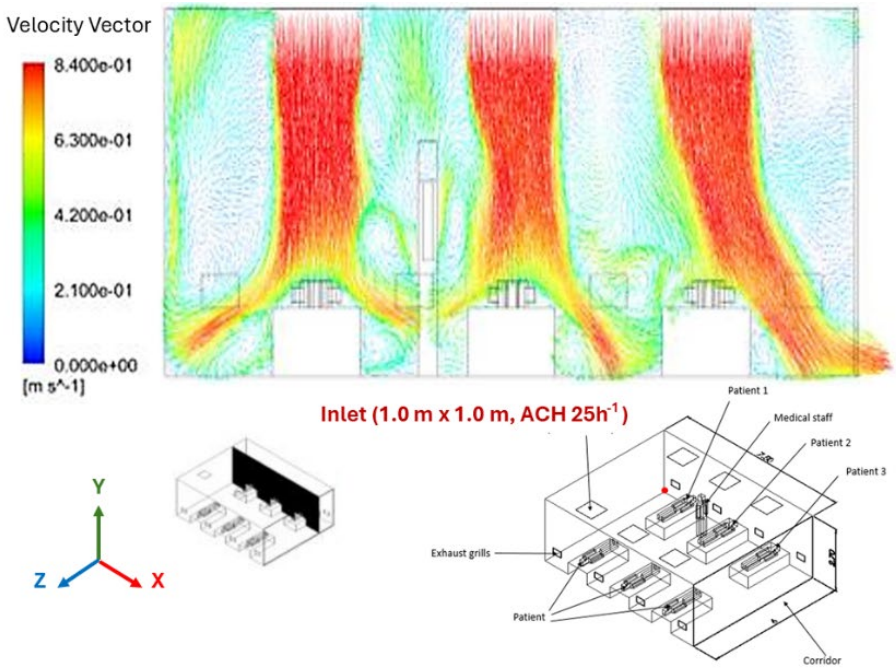

(c)

Figure 7: Airflow velocity vector plot in (a) Case 1 with ACH $9h^{-1}$, (b) Case 2 with ACH $16h^{-1}$ and (c) Case 3 with ACH $25h^{-1}$.

Figure 8 illustrates the effects of different air change rates and supply diffuser sizes on airborne particle dispersion within the patient ward. In Figure 8(a), a high particle concentration of 53 particles/m³ accumulated on Patient 1's body, while lower concentrations of 11–16 particles/m³ were observed around the head and leg areas. Additionally, some particles (11–21 particles/m³) traveled toward the front of the patient's bed and the adjacent walls on the right side, posing a risk of cross-infection to the patient positioned opposite Patient 1. The side view shows some particles being carried upwards accumulated above Patient 1. However, unlike the baseline model, airborne particles did not reach the medical staff, Patient 2, or Patient 3. Figure 8(b) shows that the dispersion of particles extended further in front of Patient 1, leading to a lower particle concentration on the patient's body, with only a small number of particles (5–11 particles/m³) detected near the medical staff and other patients. The side view shows particles were kept near the patient level reflecting limited vertical dispersion of particles. Figure 8(c) demonstrates a significant reduction in particle concentration on Patient 1's body, with airborne particle dispersion effectively contained within the patient's immediate surroundings. This containment reduces the risk of cross-infection, as no particles were observed reaching medical staff or other patients. The results confirm that an ACH of $25h^{-1}$, combined with a larger supply air diffuser size of 1 m × 1 m and an inlet velocity of 0.84 m/s, significantly improves airborne particle removal compared to the baseline case (ACH = $9h^{-1}$, supply diffuser size = 0.6 m × 0.6 m, same velocity of 0.84 m/s). The findings suggest that optimizing both the air change rate and diffuser size plays a crucial role in minimizing airborne particle transmission, thereby enhancing infection control measures within the ward.

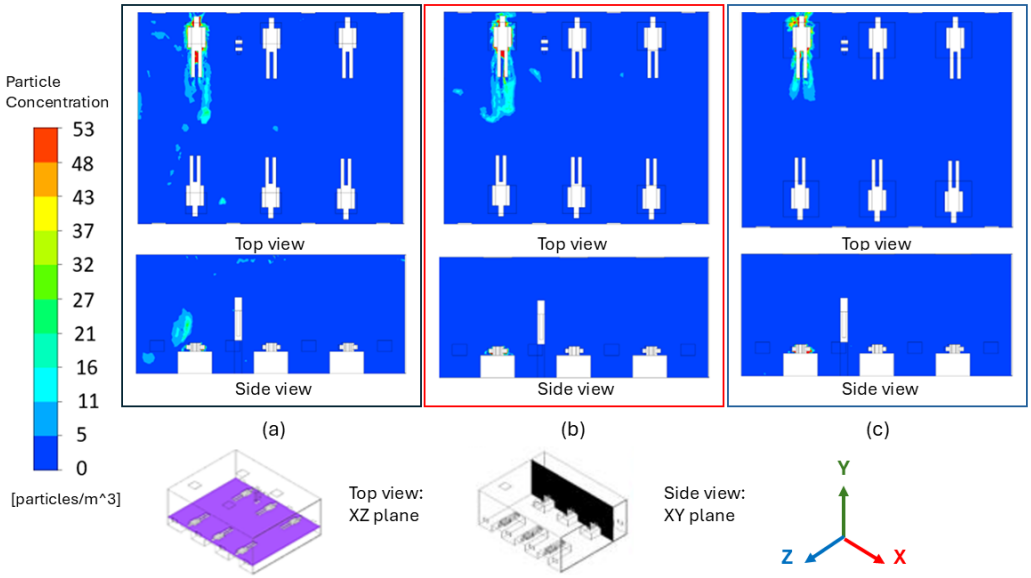

Figure 8: Particle distribution plot in (a) Case 1 with ACH $9h^{-1}$, (b) Case 2 with ACH $16h^{-1}$ and (c) Case 3 with ACH $25h^{-1}$

3.4 Summary of Result.

Previous investigations revealed that particles released from Patient 1 leads to a higher risk of cross-infections. Therefore, Figure 9 illustrates the particle concentration accumulated on the surface of Patient 1, as well as the average particle concentration on other lying patients and standing medical staff due to the particles released from Patient 1 to assess the efficiency of different supply diffuser configurations. The baseline case, with an ACH of $9h^{-1}$, showed that airborne particles from Patient 1 reached other patients and medical staff resulted in a particle concentration of 16 particles/m^3, indicating that the airflow was not effectively removing particles. Case 1, with an ACH of $9h^{-1}$ and six supply air diffuser of 0.6 m x 0.6 m, showed a slight improvement and resulted in a reduction of particle concentration on top of Patient 1 (from 37 to 16 particles/m^3) and around other patients and medical staff (from 16 to 11 particles/ m^3) compared to the baseline model. However, particles still reached other occupants. Case 2, with an ACH of $16h^{-1}$ and six supply air diffusers of 0.8 m x 0.8 m, further reduced the particle concentration on top of Patient 1 to 0 particles/ m^3 and around other particles and medical staff to 5 particles/m^3. Case 3, with an ACH of $25h^{-1}$ and six supply air diffusers of 1 m x 1 m, was the most effective in reducing the airborne particle transmission. It achieved 100% reduction in airborne particle concentration on top of Patient 1 and around other patients and medical staff compared to the baseline. This was attributed to the higher airflow velocity resulting from the increased ACH.

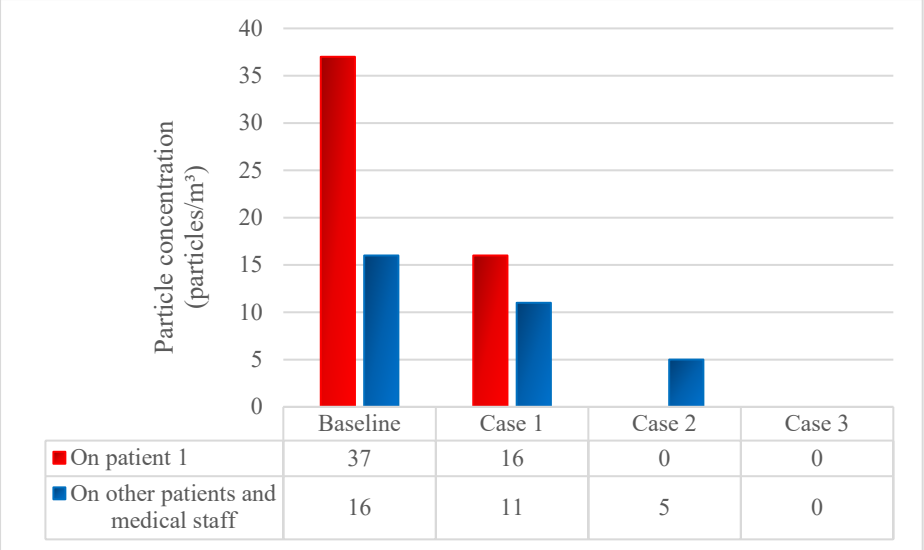

	Baseline	Case 1	Case 2	Case 3
On patient 1	37	16	0	0
On other patients and medical staff	16	11	5	0

Figure 9: Particle settlement of each case**.**

4.0 CONCLUSION

This research successfully validated an airflow turbulence model to analyse airflow distribution and particle dispersion in a patient ward using CFD. RNG k-epsilon provides a simulated result with the lowest percentage relative error (19.3%) compared to experimental data. The study demonstrated that increasing the air changes per hour (ACH) from $9h^{-1}$ to $25h^{-1}$, along with optimizing the supply air diffuser size to 1.0 m × 1.0 m, significantly reduced airborne particle concentration. Specifically, at ACH = $25h^{-1}$, airborne particle concentration was reduced by 100% above Patient 1 and throughout the surrounding areas, minimizing the risk of cross-contamination among patients and medical staff. The results highlighted that a higher ACH enhances particle removal, thereby improving indoor air quality and infection control. However, residual airborne particles at lower heights, particularly near the patient's legs, suggest that further refinement of airflow distribution is necessary to prevent potential resuspension due to movement. Future research should explore transient conditions by incorporating dynamic interactions, such as medical staff movement, to further enhance the accuracy and applicability of the findings. Additionally, optimizing ventilation strategies to balance airflow velocity and patient comfort remains a crucial consideration for real-world implementation.

ACKNOWLEDGEMENT

The authors would like to acknowledge the financial support from Asia Technological University (ATU) Network under ATU-Net Young Researcher Grant (YRG) with Vot. No. R.J130000.7724.4J714and Universiti Teknologi Malaysia under UTM Nexus Postgrad with Vot no. Q.J130000.5324.00L96. Also, the authors acknowledge UTM PROSPECT centre for providing access to the Ansys Fluent software and desktop facilities that were essential to the successful completion of this study.

REFERENCES

1. Casagrande, D. and M. Piller, *Conflicting effects of a portable ultra-clean airflow unit on the sterility of operating rooms: A numerical investigation.* Building and Environment, 2020. **171**: p. 106643. DOI: https://doi.org/10.1016/j.buildenv.2020.106643.
2. Sheng, S., et al., *Performance of all-air wall induction unit for displacement ventilation in a four-bed hospital ward during the cooling period.* Building and Environment, 2024. **248**: p. 111101. DOI: https://doi.org/10.1016/j.buildenv.2023.111101.
3. Magill, S.S., et al., *Multistate point-prevalence survey of health care-associated infections.* New England Journal of Medicine, 2014. **370**(13): p. 1198-1208.DOI: 10.1056/NEJMoa1306801.
4. Giannini, M.A., D. Nance, and J.A. McCullers, *Are toilet seats a vector for transmission of methicillin-resistant Staphylococcus aureus?* American Journal of Infection Control, 2009. **37**(6): p. 505-506.DOI: 10.1016/j.ajic.2008.11.005.
5. Morawska, L. and J. Cao, *Airborne transmission of SARS-CoV-2: The world should face the reality.* Environment International, 2020. **139**: p. 105730. DOI: https://doi.org/10.1016/j.envint.2020.105730.
6. Spilchuk, V., V.H. Arrandale, and J. Armstrong, *Potential risk factors associated with COVID-19 in health care workers.* Occup Med (Lond), 2022. **72**(1): p. 35-42. DOI: 10.1093/occmed/kqab148.
7. Fu, Y., et al., *Inhalation exposure assessment techniques on ventilation dilution of infectious respiratory particles in a retrofitted hospital lung function room.* Building and Environment, 2023. **242**: p. 110544. DOI: https://doi.org/10.1016/j.buildenv.2023.110544.
8. Ibrahim, F., et al., *Hospital indoor air quality and its relationships with building design, building operation, and occupant-related factors: A mini-review.* Frontiers in Public Health, 2022. **10**.
9. Xu, et al., *The 2019-nCoV epidemic control strategies and future challenges of building healthy smart cities.* Indoor and Built Environment, 2020. **29**(5): p. 639-644.DOI: 10.1177/1420326X20910408.
10. Fan, X.-Y., et al., *More obvious air pollution impacts on variations in bacteria than fungi and their co-occurrences with ammonia-oxidizing microorganisms in PM2.5.* Environmental Pollution, 2019. **251**: p. 668-680. DOI: https://doi.org/10.1016/j.envpol.2019.05.004.
11. Palladino, G., et al., *Particulate matter emission sources and meteorological parameters combine to shape the airborne bacteria communities in the Ligurian coast, Italy.* Scientific Reports, 2021. **11**: p. 12.DOI: 10.1038/s41598-020-80642-1.
12. Li, Y., et al., *Role of air distribution in SARS transmission during the largest nosocomial outbreak in Hong Kong.* Indoor air, 2005. **15**: p. 83-95.DOI: 10.1111/j.1600-0668.2004.00317.x.
13. Kupferschmidt, K., *Did poor ventilation lead to MERS 'superspread' in Korea?* Science, 2015.DOI: 10.1126/science.aac6802.
14. Tan, H., et al., *Why do ventilation strategies matter in controlling infectious airborne particles? A comprehensive numerical analysis in isolation ward.* Building and Environment, 2023. **231**: p. 110048. DOI: https://doi.org/10.1016/j.buildenv.2023.110048.
15. Tan, H., et al., *Systematic study on the relationship between particulate matter and microbial counts in hospital operating rooms.* Environmental Science and Pollution Research, 2022. **29**(5): p. 6710-6721.DOI: 10.1007/s11356-021-16171-9.
16. Berríos-Torres, S.I., et al., *Centers for Disease Control and Prevention Guideline for the Prevention of Surgical Site Infection, 2017.* JAMA Surgery, 2017. **152**(8): p. 784-791.DOI: 10.1001/jamasurg.2017.0904.
17. Islam, M.T., et al., *Effects of recirculation and air change per hour on COVID-19 transmission in indoor settings: A CFD study with varying HVAC parameters.* Heliyon, 2024. **10**(15): p. e35092. DOI: https://doi.org/10.1016/j.heliyon.2024.e35092.
18. Bolashikov, Z.D., et al., *Exposure of health care workers and occupants to coughed airborne pathogens in a double-bed hospital patient room with overhead mixing ventilation.* Hvac&r Research, 2012. **18**: p. 602-615.DOI: 10.1080/10789669.2012.682692.
19. Ghia, U., et al., *Assessment of Health-Care Worker Exposure to Pandemic Flu in Hospital Rooms.* (0001-2505 (Print)).
20. Stockwell, R.E., et al., *Indoor hospital air and the impact of ventilation on bioaerosols: a systematic review.* Journal of Hospital Infection, 2019. **103**(2): p. 175-184. DOI: https://doi.org/10.1016/j.jhin.2019.06.016.
21. Noorimotlagh, Z., et al., *A systematic review of possible airborne transmission of the COVID-19 virus (SARS-CoV-2) in the indoor air environment.* Environmental Research, 2021. **193**: p. 110612. DOI: https://doi.org/10.1016/j.envres.2020.110612.
22. Taghinia, J.H., M.M. Rahman, and X. Lu, *Effects of different CFD modeling approaches and simplification of shape on prediction of flow field around manikin.* Energy and Buildings, 2018. **170**: p. 47-60. DOI: https://doi.org/10.1016/j.enbuild.2018.03.075.
23. Satheesan, M.K., K.W. Mui, and L.T. Wong, *A numerical study of ventilation strategies for infection risk mitigation in general inpatient wards.* Building Simulation, 2020. **13**(4): p. 887-896.DOI: 10.1007/s12273-020-0623-4.
24. Kamar, H.M., K.Y. Wong, and N. Kamsah, *The effects of medical staff turning movements on airflow distribution and particle concentration in an operating room.* Journal of Building Performance Simulation, 2020. **13**(6): p. 684-706.DOI: 10.1080/19401493.2020.1812722.

25. Nielsen, C. and P. Martins, *Finite element simulation: a user's perspective.* Metal forming: formability, simulation and tool design. Academic Press, London. https://doi. org/10.1016/B978-0-323-85255-5.00011-X, 2021.
26. Zou, D., et al., *An enhanced octree polyhedral scaled boundary finite element method and its applications in structure analysis.* Engineering Analysis with Boundary Elements, 2017. **84**: p. 87-107. DOI: https://doi.org/10.1016/j.enganabound.2017.07.007.
27. Wijesooriya, K., et al., *A technical review of computational fluid dynamics (CFD) applications on wind design of tall buildings and structures: Past, present and future.* Journal of Building Engineering, 2023. **74**: p. 106828. DOI: https://doi.org/10.1016/j.jobe.2023.106828.
28. Kek, H.Y., et al., *Evaluating the impact of human movement-induced airflow on particle dispersion: A novel real-time validation using IoT technology.* Energy and Buildings, 2024. **323**: p. 114825. DOI: https://doi.org/10.1016/j.enbuild.2024.114825.
29. Wu, et al., *Numerical study of transient indoor airflow and virus-laden droplet dispersion: Impact of interactive human movement.* Science of The Total Environment, 2023. **869**: p. 161750. DOI: https://doi.org/10.1016/j.scitotenv.2023.161750.
30. Tan, H., et al., *Does human movement-induced airflow elevate infection risk in burn patient's isolation ward? A validated dynamics numerical simulation approach.* Energy and Buildings, 2023. **283**: p. 112810. DOI: 10.1016/j.enbuild.2023.112810.
31. Tan, H., et al., *Controlling infectious airborne particle dispersion during surgical procedures: Why mobile air supply units matter?* Building and Environment, 2022. **223**: p. 109489. DOI: https://doi.org/10.1016/j.buildenv.2022.109489.
32. Tan, H., et al., *Current and potential approaches on assessing airflow and particle dispersion in healthcare facilities: a systematic review.* Environmental Science and Pollution Research, 2022. DOI: 10.1007/s11356-022-23407-9.
33. Sadeghian, P., *Computational fluid dynamics application in indoor air quality and health*. 2022, KTH Royal Institute of Technology.
34. Yang, C., X. Yang, and B. Zhao, *The ventilation needed to control thermal plume and particle dispersion from manikins in a unidirectional ventilated protective isolation room.* Building Simulation, 2015. **8**(5): p. 551-565. DOI: https://10.1007/s12273-014-0227-6.